VHF Antenna Far-Field Pattern Measurements at 60 MHz Using an Outdoor Antenna Range for Europa Clipper Mission

Joshua M. Miller, Yasser Hussein, Curtis Jin, Emmanuel Decrossas

***Abstract*—Improvements to measurements of a VHF folded dipole operating at 55-65 MHz to be used as part of a radar for a mission to one of Jupiter's moons, Europa, are presented. Previous measurements using an unmanned aerial vehicle (UAV) or small unmanned aerial system (sUAS) are improved upon by reducing systematic errors and more accurately tracking distances within the measurement system on an outdoor measurement range at Jet Propulsion Laboratory (JPL). Details of the measurement system setup are presented along with a brief discussion of error sources. Comparing previously collected measurement data with the new measurements reveal an improvement of approximately 0.4 dB in accuracy with an improvement in over 1 dB for error budgets.**

***Index Terms*—Europa, far-field, Very-High Frequency, VHF, NASA, radiation pattern, antenna range, outdoor antenna measurements.**

I. Introduction

Onboard the National Aeronautics and Space Administration's (NASA) upcoming mission, Europa Clipper, to Jupiter's moon Europa, the Radar for Europa Assessment and Sounding: Ocean to Near-surface (REASON) instrument is a dual-band, sounding radar operating in the Very-High Frequency (VHF) band centered at 60 MHz and in the High-Frequency (HF) band centered at 9 MHz. REASON will remotely map ice coverage of the surface of Europa, one of Jupiter's moons, while orbiting. For each band of operation, antenna arrays made up of dipole approximately one-half wavelength in length are used for both transmit and receive of the radar signals. These antennas for the radar instrument must accurately be characterized to enable high quality measurements of the surface of this remote and icy world. This manuscript focuses on the measurements and characterization of the VHF antennas Radio Frequency (RF) performance for this mission.

The research described herein was carried out at the Jet Propulsion Laboratory, California Institute of Technology. U.S. Government sponsorship acknowledged.

J. M. Miller is part of the Flight Communications Section at the NASA Jet Propulsion Laboratory, California Institute of Technology, Pasadena, CA 91109 USA. (e-mail: Joshua.M.Miller@jpl.nasa.gov).

Y. Hussein is part of the Flight Communications Section at the NASA Jet Propulsion Laboratory, California Institute of Technology, Pasadena, CA 91109 USA. (e-mail: Yasser.A.Hussein@jpl.nasa.gov).

C. Jin is part of the Flight Communications Section at the NASA Jet Propulsion Laboratory, California Institute of Technology, Pasadena, CA 91109 USA. (e-mail: Curtis.Jin@jpl.nasa.gov).

E. Decrossas is part of the Flight Communications Section at the NASA Jet Propulsion Laboratory, California Institute of Technology, Pasadena, CA 91109 USA. (e-mail: Emmanuel.Decrossas@jpl.nasa.gov).

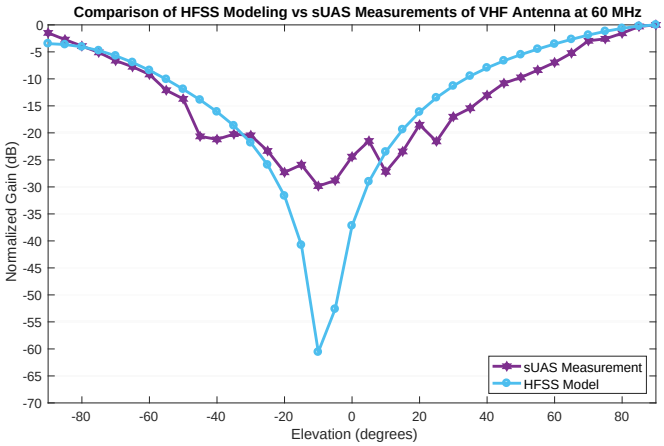

Fig. 1. Simulated and measured normalized gain comparison using several independent measurements of the same cut to estimate the repeatability error for elevation cut of VHF antenna over ground plane using the sUAS measurement system.

Typical methods for measuring antennas, such as measurements in anechoic chambers, are often difficult to perform for antennas operating in the VHF range between 30 MHz to 300 MHz due to the long wavelengths associated. While antennas that operate at Ultra-High Frequencies (300 MHz to 3 GHz) and above can be measured in an indoor antenna range, most indoor ranges are not equipped to provide adequate isolation for measurement at VHF frequencies where wavelengths can exceed 1 meter. To provide a quiet zone (QZ) at frequencies below 300 MHz, it is necessary to use carbon impregnated pyramid absorbers in excess of 6 to 8 ft (1.8 m to 2.4 m) in height paired with ferrite tiles to ensure an adequate RF environment inside the anechoic chamber. When combined, these absorbers and tiles can exceed 215 kg/m^2 in mass and would require a room of over 6 m in height to provide a working space of 2 m with absorber on the floor and ceiling. The sheer physical size and weight of these absorbers necessary to get return losses low enough for acceptable pattern measurements are restricted from use in all but the largest of anechoic chambers.

As this kind of measurement space was not readily available, the Jet Propulsion Laboratory opted to extend their capabilities for lower frequency antennas and develop measurement techniques to perform these measurements at 60 MHz using the outdoor antenna range at JPL.

II. Previous Measurements

Prior to the measurements described in this paper, experimental measurements for a 60 MHz dipole at an Open

Fig. 2. Satellite view of the mesa antenna measurement facility at JPL and the outdoor range (highlighted) used for measuring VHF antennas at 60 MHz

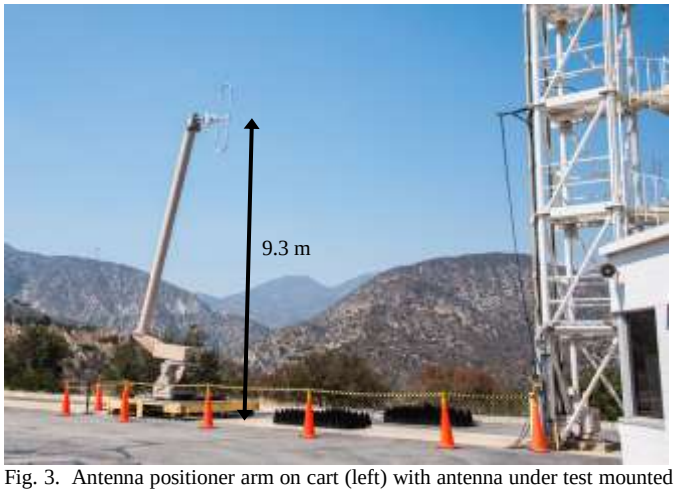

Fig. 3. Antenna positioner arm on cart (left) with antenna under test mounted on top facing the fixed tower (right).

Area Test Site (OATS) in Kimballton, Iowa using a dipole mounted above a large 50 m × 70 m (3500 m^2) ground plane were performed. A small unmanned aerial system/unmanned aerial vehicle (sUAS/UAV) equipped with a receiver and measurement antenna flew a prescribed path around the antenna under test (AUT) to collect field strength measurements. [1][2]

The VHF folded dipole over a ground plane was modeled using both HFSS[3] and EZNEC[4]. The results of the simulations were compared against the data collected with the sUAS.

While the results agree closely as seen in Figure 1, the delta between the measured and simulated peak boresight gain of the antenna is approximately 0.91 dB. The resulting total systematic error of the measurement setup using an sUAS over the ground plane is estimated ± 2 dB.

III. Test Facility and Space

While the initial measurements of the VHF dipole proved to be successful, it was decided to pursue additional measurements on-site at JPL to enable faster turn around of data and antenna measurements during winter seasons.

The JPL facility has two indoor anechoic chambers equipped with near and far field measurement capabilities up to 100 GHz and beyond. Also available at the facility are three outdoor antenna measurement ranges. The facility is situated on a mesa (a flat-topped hill) above the main JPL campus, as seen in Figure 2, and provides an attractive environment for antenna measurements as the immediate surrounding terrain is well below the hilltop, which provides a relatively reflection-free environment for outdoor measurements in the UHF and above range.

The west range consists of a fixed metal tower approximately 12 m in height with a movable sled that can be moved vertically up and down the tower to adjust the height relative to the ground. Across from the fixed tower is a movable cart on tracks with a fiberglass support arm and roll positioner on top of the arm (Figure 3). The support arm is remotely controllable to change elevation angle and also azimuth angle relative to the fixed tower. The support arm can be raised to a maximum height of 9.3 m above the ground. While the metal tower is fixed, the cart with positioner on tracks can be moved to allow for up to 40 m of separation between the two antenna mounting points on the two structures as shown in Figure 4.

To measure the VHF folded dipoles on the range as depicted in Figure 3, the antenna under test (AUT) or transmitter is mounted onto the roll positioner on top of the arm on the movable cart. This configuration permits the AUT to be positioned in any angle with respect to the fixed tower for measurements of the antenna pattern.

Opposite of the AUT on the fixed tower, mounted on the movable sled, is an active electric field probe used for measuring the electrical field radiated from AUT providing continuous coverage from 9 kHz to 300 MHz.[5]

Once mounted, the fiberglass arm of the movable cart is raised to the maximum height of 9.3 m and the field probe raised to be in line of sight of the AUT.

In order to ensure that we are operating the AUT in the far field of the antenna, we use the standard equation for the far field boundary in free space (Eq. 1).

$$L < 0.62\sqrt{\frac{D^3}{\lambda}} \tag{1}$$

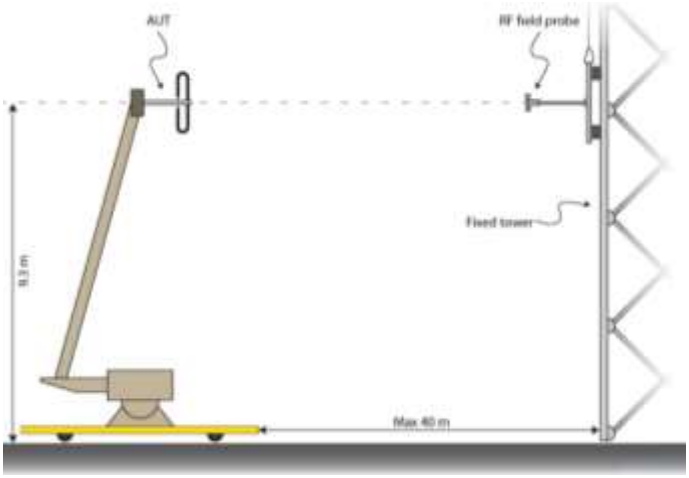

Fig. 4. Configuration of the outdoor measurement range with the movable cart and antenna positioner on the left and the fixed tower on the right.

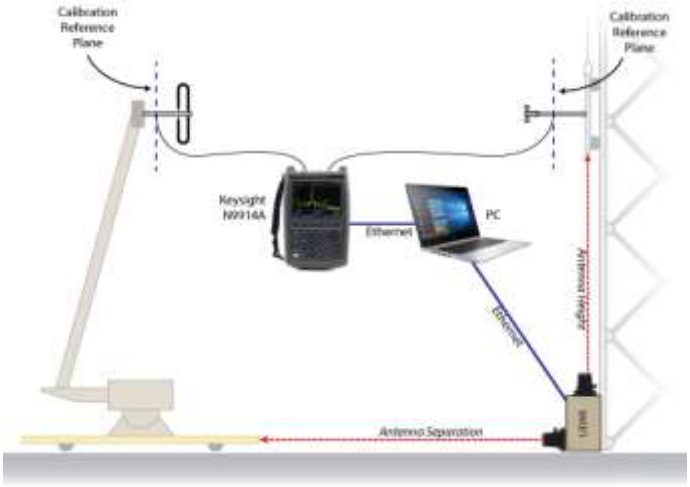

Fig. 5. Connections of hardware on the antenna range for automation of measurements and data collection

However, since we are operating over the ground and not in an anechoic chamber or an environment that approaches free space, we must consider the effect of the ground where it generates a virtual image of the AUT. To account for this image antenna, we multiply the original equation by a factor of 2 and form Equation 2.

$$L < (2)(0.62)\sqrt{\frac{D^3}{\lambda}} \qquad (2)$$

Using D = 2.5 m, which is the maximum dimension of our antenna, and λ = 5 m, the resulting far field boundary is calculated as 2.19 m. By placing the AUT at the maximum height of 9.3 m over the ground, we ensure the ground is outside of the far field region.

To collect the data, a portable network analyzer is used to perform a full two-port measurement. The AUT is connected to port 1 of the analyzer while the measurement probe is connected to port 2. Prior to connecting the antennas to the coaxial cables on the towers, a full 2-port calibration using an open, short, load, and through measurement is performed at the ends of the cables, which connect to the AUT and probe. By doing this, the reference place of the network analyzer is electrically extended outward from the analyzer to the antennas in the test setup, eliminating any cable and connector losses from the measurement. This essentially allows us to directly measure antenna gain and path losses along with phase information as the antenna moves. By performing an S_{21} measurement with the analyzer after the calibration, we are measuring the response of the antenna system without any system path loss. Further, the probe and AUT are aligned perfectly to ensure zero polarization loss. The distances between antennas and the height of the antennas from the ground are tracked so that the changes in magnitude and phase can be properly correlated. A light detection and ranging (LIDAR) measurement system was developed to enable accurate and automated collection of the distances within the system. Using commercial off the shelf (COTS) LIDAR modules paired with a Raspberry Pi, we are able to achieve measurements up to 40 m with an accuracy of ±2.5 cm.[6] These LIDAR sensors communicate over an I^2C bus with the Raspberry Pi where custom Python software was written to continuously query the sensors for measurements and log measurement data. The software also permits entry of mounting offsets and static deltas to make post-measurement calculations easier.

To further automate data collection and processing, a PC is connected to the network analyzer and the LIDAR controller through an ethernet connection. A Python scripts allow S-parameters of the system versus distance between antennas to be continuously or selectively recorded.

IV. Multipath Effects and Correlation

Prior to performing any antenna pattern measurements, the effects of multipath are studied on the range. Since we are operating over a lossy ground and not in a free space environment, it is expected that there will be constructive and destructive interferences due to reflections from ground.[7]

In order to measure these effects, the range is configured as it would normally be for a far-field radiation pattern measurement with the AUT mounted on the movable arm of the positioner cart and the RF field probe mounted on the fixed tower.

Each antenna is raised to the same height of 9.3 m and the cart is moved to the maximum distance of 26 m. For this initial measurement, cable length was a limiting factor for antenna separation. It's worth noting that the 9.3 m height was chosen such that there is a direct line-of-sight (LOS) between the AUT and probe. This will ensure zero obstruction and no loss of energy due to RF signal blocking.[8]

The antennas are mounted in horizontal polarization to position the main lobe of the antennas towards the ground. For vertical polarization, the antenna pattern should be considered as the look angle to the center reflection point on the ground changes with distance. In addition, horizontal polarization is preferred for antenna measurements since the mutual coupling between the antenna and the orthogonal ground is negligible. Horizontal calculations are much simpler than the vertical polarization calculations due to the horizontal ground wave being less sensitive to the differences in surface conductivity and permittivity compared to the vertical wave.[9]

After the antenna is mounted horizontally, the cart is slowly

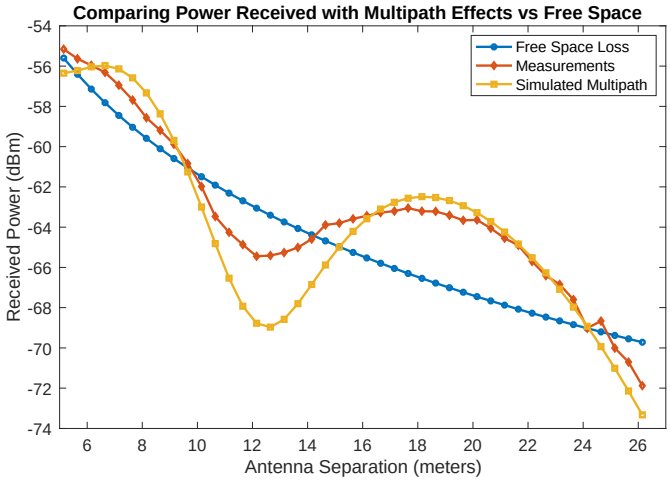

Fig. 6. Antenna spacing versus received power for optimizing locations to minimize multi-path effect at 60 MHz for horizontal polarization.

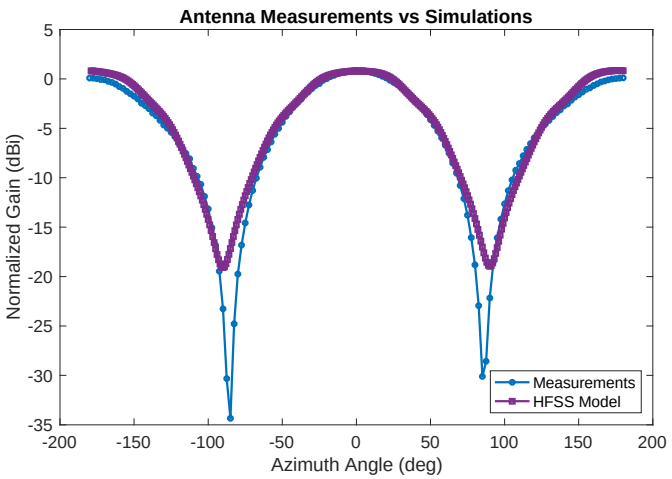

Fig. 7 Comparison of HFSS model and actual measurements of the VHF antenna on the outdoor antenna range at 60 MHz.

pushed forward towards the fixed tower, decreasing the antenna separation from 26 m to 5 m. While the cart is being moved, the automated collection system using the LIDAR, network analyzer, and networked PC is used to continually log and collect path loss data (S_{21} measurements) versus distance between the AUT and the RF field probe. This process is repeated to collect multiple sets of data for statistical analysis.

The collected data is then compared against a path loss versus distance for both free space and over a lossy ground plane using the two-ray model[10] as seen in Figure 6. When the two-ray model simulation, real measurements, and free-space loss intersect on the graph, minimal multipath effects are achieved. For this case of the two antennas operating horizontally at 60 MHz, all three intersect at 9.65 m and 24.1 m, providing two points to place the AUT for measurements with minimal multipath effects present. The separation distance of 24.1 m is chosen to ensure operation in the far field of the antenna and to further reduce any interaction of the AUT and fixed tower. Also, choosing the larger separation distance minimizes errors due to amplitude as well as phase tapers.

V. Antenna Pattern Measurements

To measure the radiation pattern, the AUT is mounted on the antenna positioner on the movable cart and the cart moved to provide a separation of 24.1 m between the two antennas. A full 2-port calibration on the network analyzer is performed at the connection points to each the AUT and the measurement probe prior to connecting the antennas.

Automated co-polarization measurements are performed to collect the S_{21} values versus antenna angular positions at 1-degree intervals. These S_{21} values are then translated into antenna gain factors based on the known gain of the measurement probe.

Comparing the measurements with the simulations, one can see that both sets of data follow the same trends and track well. At the main lobe of the antenna on boresight, the delta between the measured value and the simulation value from HFSS is 0.5 dB – approximately a 0.4 dB improvement over measuring the antenna on the OATS with the sUAS.

By controlling positional errors more closely (e.g. fixed antennas with high-precision distance measurements and no sUAS) systematic error has been reduced to roughly ±0.86 dB (1 σ) for these measurements at 60 MHz, with the largest source of error coming from the measurement probe with ±0.8 dB.

Acknowledgements

The authors would like to thank and acknowledge Jefferson Harrell and Tom Musselman for their contributions to our development of these antenna measurements. Their continued support through discussion and analysis to improve the measurement techniques has been invaluable.

Conclusions

By reducing the amount of physically moving pieces of a system and carefully considering multipath effects, it possible to perform accurate measurements at low VHF (< 100 MHz) frequencies with outdoor space. Results show that an antenna operating at 60 MHz over a lossy, outdoor ground plane can be characterized and match simulations within 1 dB. While performing these pattern measurements outdoors using an OATS with a sUAS measurement system can be done, it is shown that more accurate measurements can be collected over a lossy ground plane when considering all setup factors.

References

[1] Y. Hussein, J. Miller, V. Garkanian, and E. Decrossas, "Far-Field Pattern Measurement and Simulation of VHF Antenna at 60 MHz for Europa Clipper mission", in *IEEE Symposium on Electromagnetic Compatibility, Signal Integrity and Power Integrity*, Long Beach, CA, 2018, p. 94-98.

[2] "Far-Field Radiation Pattern Measurements of High-Frequency Antennas with Unmanned Aerial Systems," U.S. Provisional Pat. Ser. No. 62/560,797, filed September 20, 2017.

[3] Ansys HFSS, Pittsburgh, PA, Version 15.0.0, 2012.

[4] NEC, Version 5.8.16, 2015.

[5] Schwartzbeck Mess-Elektronik. (April, 2019). *Active Electric Field Probe with Biconical Elements and Built-in* Amplifier [Online]. Available: http://www.schwarzbeck.de/Datenblatt/m9218.pdf

[6] Garmin Ltd. (April, 2019). *LIDAR-Lite v3HP Operation Manual and Technical Specifications* [Online]. Available: http://static.garmin.com/pumac/LIDAR-Lite_v3HP_Instructions_EN.pdf

[7] Smith, A. A., Jr., "Standard site method for determining antenna factors," IEEE Transactions on Electromagnetic Compatibility, EMC-24, pp. 316-322, no. 3, Aug. 1982.

[8] Warren L. Stutzman and Gary A. Thiele, Chapter 13. Antenna Theory and Design. Third Edition. John Wiley and Sons Inc. 2012.

[9] A. C. Newell, R. C. Baird, and P. F. Wacker, "Accurate Measurement of Antenna Gain and Polarization at Reduced Distances by an Extrapolation Technique", *IEEE Transactions on Antennas and Propagation*, vol AP-21, July 1973, pp 418—431.

[10] Loyka, Sergey; Kouki, Ammar (October 2001). "Using Two Ray Multipath Model for Microwave Link Budget Analysis". *IEEE Antennas and Propagation Magazine*. 43 (5): 31–36.